Regular Paper

Slotted Implantable Patch Antenna for ISM Band Application and Its Usage in WiMAX with an I-Shaped Defected Ground Structure

Adil Al Ayubi[a,†], Shikha Sukhija[b,†], and Rakesh Kumar Sarin

Department of Electronics and Communication Engineering, DR. B. R. Ambedkar National Institute of Technology, Jalandhar 144011, India

A slotted implantable patch antenna with microstrip feeding is proposed for industrial, scientific, and medical band applications. The result is verified by implanting the antenna in animal tissue. Further, by varying the ground width and introducing a defect into the ground structure, the antenna becomes applicable for worldwide interoperability for microwave access operations. A simulation is performed using Empire XCcel software. An Agilent vector network analyzer is used for analyzing the return loss performance. Simulated and measured results are compared. Antennas with and without defected ground structure both have key advantages including low profile, desirable return loss, good impedance matching and required bandwidth.

Keywords : Microstrip feed, Implantable antenna, ISM band, Defected ground structure, WiMAX

1. INTRODUCTION

As technology advances, the use of radio and microwave frequencies in biomedical applications has surpassed the implementation challenges and is thus becoming more widespread. Implantable antennas can communicate wirelessly with an external device to be used in patient monitoring, diagnosis, disease prevention, pacemakers, cardioverter defibrillators, blood glucose sensors, and retinal implants [1].

The United States Federal Communication Commission (FCC) and the European Communication Commission (ERC) have approved the frequency bands for implanted antennas. These frequency bands are the Medical Implanted Communication Service (MICS) band (402~405 MHz) [4] and the Industrial Scientific and Medical (ISM) band (2.4~2.5 GHz). The MICS band has a lower frequency and results in larger antenna size with low losses. In contrast, the ISM band, having a higher frequency, results in smaller antenna size with

high losses [2]. In [3], a circularly polarized microstrip patch antenna was designed for implantation. The results were obtained in skin phantom and a Gustav voxel human body. In [4], researchers opted for planar inverted-F antennas (PIFAs) for implantation purpose owing to their simple structure and compact size. In [5], an experimental setup was designed for monitoring the skin temperature of a pig through an implanted device consisting of an antenna, a battery, and biosensors.

Because implantation of an antenna in the human body requires compactness in size for remote health monitoring, the ISM band is opted for here and with an operating frequency of 2.47 GHz is chosen. The simulation is done using Empire XCcel 5.51 software, which is based on the finite-difference time domain (FDTD) method. The FDTD method is a numerical analysis technique for finding approximate solutions to differential equations. It is a time-domain analysis and can cover a wide frequency range with a single simulation run [6].

The hardware for the proposed antenna is implemented and the results are verified using an Agilent vector network analyzer. Basically, three different results are analyzed. First, simulated results are obtained through software, second, the experimental results in free space are verified. Third the antenna is inserted into chicken tissue and the results are compared. Little degradation is observed, as the antenna is dipped into the chicken tissue, which has a high

---

† Author to whom all correspondence should be addressed:
E-mail: a: adilalayubi@gmail.com, b: shikhasukhija@yahoo.co.in

dielectric loss factor [7].

Finally, the ground width of the proposed antenna is decreased slightly and an I-shaped defect is introduced in the ground plane. Owing to this vertical I-shaped defect in the ground plane, slow wave factor increases [8]. This increase in the slow wave factor implies a longer electrical length of current- is required for the same physical length. This defect in the ground plane can be converted to an LC or RLC equivalent circuit. The performance of the defected ground structure (DGS) cannot be fully predicted until the optimized results are achieved through trial and error [9]. Here also a trial and-error iterative process is followed and the result is obtained for a particular defected shape, which covers 3.5 GHz frequency with a large bandwidth and can be used for worldwide interoperability for microwave access (WiMAX) application [10].

This paper is organized as follows. In Section II, a detailed configuration of the proposed antenna for ISM band application is given. Section III introduces DGS with some predefined formulas for calculating parameters of the unit cell DGS equivalent circuit. Section IV shows the simulated and experimental results of the implantable antenna and its effect when DGS in the ground plane is introduced. Antennas with and without DGS are found to be suitable for WiMAX and biomedical applications, respectively. Finally, conclusions are given in Section V.

2. GEOMETRICAL VIEW OF ANTENNA DESIGNED FOR IMPLANTATION

The structure of the proposed antenna is shown in Fig. 1. A slotted shape patch is taken for miniaturization of the antenna as it is an essential requirement for implantation. Other shapes of patches such as crooked and spiral can also be used [4]. Introducing slots on the patch increases the current flow path. As a result, the amount of current flow increases and overall parameters, i.e., return loss, 3 dB bandwidth and radiation pattern of the antenna improve [11]. Because microstrips are easy to fabricate and offer good impedance
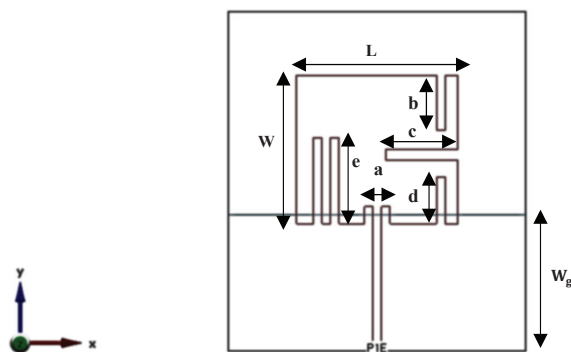
matching, microstrip feeding is provided for this proposed structure A partial ground structure is chosen as it somewhat improves the operating frequency range of the antenna found through simulation. The footprint of the proposed antenna is 35 × 40 × 1.6 mm and the other details of the configuration are listed in Table 1. A cheap and easily available FR4 substrate having a permittivity equal to 4.4, tanδ = 0.002 and a thickness of 1.6 mm is used for prototyping of the antenna.

3. INTRODUCING I-SHAPED DGS

The proposed structure is designed to operate in the 3.75 GHz frequency band. A number of simulations are conducted in which the dimensions were varied. Choosing the same structure, except changing the ground width from 16 to 12 mm and inserting an I-shaped DGS, leads to applicability to WiMAX with a large bandwidth.

An enormous increase in bandwidth is achieved by varying the width of the ground plane. The ground width is changed iteratively for optimizing the result. An antenna with an I-shaped defect in the ground plane is shown in Fig. 2 and its detailed configuration is described in Table 2. Figure 3 illustrates the geometrical view of the I-shaped DGS.

In general, the unit cell DGS equivalent is a parallel tuned circuit in series with the transmission line to which it is coupled, [12] as shown in Fig. 4. The two rectangular parts of the I-shaped DGS stores inductance and the slots used in between the two rectangular part store capacitance. As a result effective capacitance and inductance increase and resonance occurs at a particular frequency owing to the parallel LC circuit. Radiation, and other losses are equivalently given by resistance. Most of the DGSs have the same equivalent circuit of parallel RLC components connected in series with the transmission line [13] and play the same role. The change in type of DGS is only provided to improve the performance of the antenna. The dimensions given for a particular DGS can be used to calculate the equivalent *R, L* and *C* values from the following expressions [9].
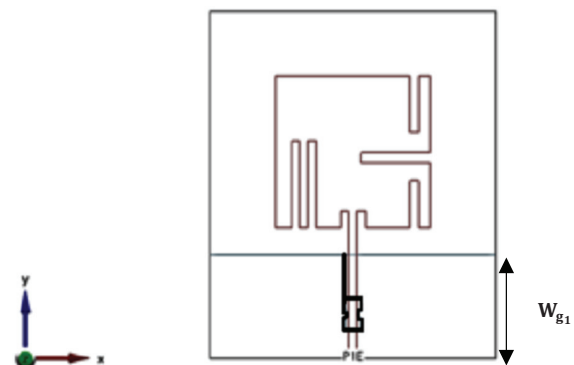

Fig. 1. Geometrical view of the proposed antenna.

Table 1. Optimal parameters of the antenna for implantation.

Parameter	Dimension (mm)
W	17.5
L	15
w_g	16
a	1
b	6.5
c	8.5
d	5.5
e	10.1

Fig. 2. Geometrical view of the proposed antenna with DGS.

Table 2. Optimal parameters of the antenna with DGS.

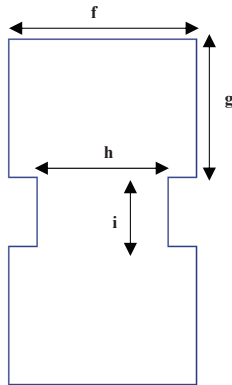| Parameter	Dimension (mm)
W_{g1}	12
f	2
g	1.5
h	1.4
i	0.75

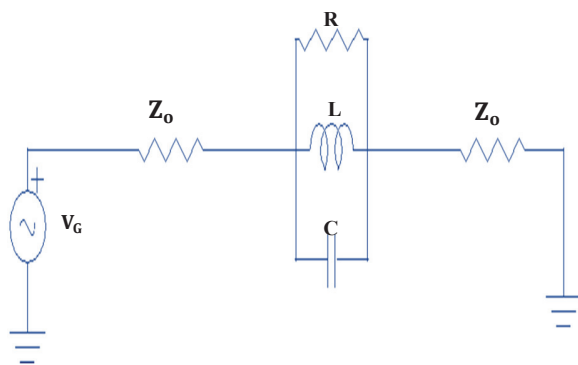Fig. 3. Geometrical view of the proposed defected ground structure.

Fig. 4. Equivalent circuit of unit cell DGS.

$$C = \frac{\omega_c}{2Z_o\left(\omega_o{}^2 - \omega_c{}^2\right)}$$

$$L = \frac{1}{4\pi^2 f_o{}^2 C}$$

$$R\left(\omega\right) = \frac{2Z_o}{\sqrt{\frac{1}{|s_{11}(\omega)|^2} - \left(2Z_o\left(\omega C - \frac{1}{\omega L}\right)\right)^2 - 1}}$$

where, ω_0 and ω_c are the resonance and angular cutoff frequencies respectively which can be calculated from an electromagnetic simulation.

4. RESULTS AND ANALYSIS

This section describes the experimental results and its comparison with the simulated ones.

4.1 Result verification using an agilent network analyzer

Experimental results should be evaluated to analyze their variation from simulation results. Figure 5 shows the hardware of the proposed antenna which is fabricated using an EP 2002 series PCB prototyping machine. To measure the performance of the implanted antenna in a realistic environment, the antenna is dipped into a rectangular shaped box having chicken tissue, which has some dielectric loss. The dimensions of the box are 100 × 100 × 24 mm. The results for the antenna in this chicken tissue obtained using an Agilent vector network analyzer (model N5230A) (10 MHz~20 GHz) at room temperature [14,15] are shown in Fig. 6.
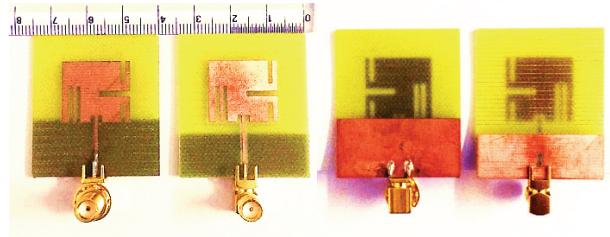

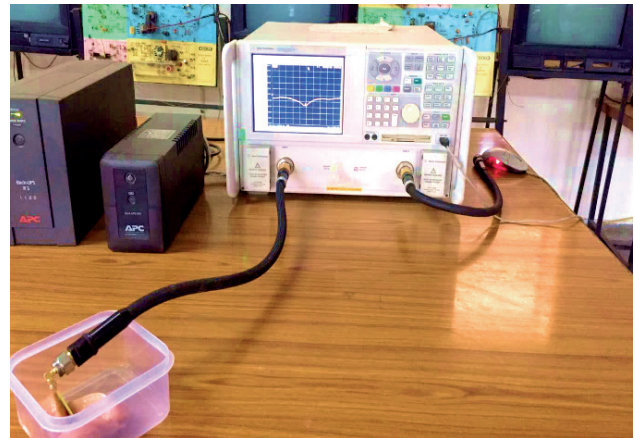Fig. 5. Hardware implementation of proposed antennas.

Fig. 6. Experimental result of the proposed antenna in a chicken tissue using VNA.

4.2 Comparative S parameter vs frequency curves

The scattering parameter S defines the return loss of an antenna which should be, ≤ -10 dB. Here, the return loss of nearly -16 dB is achieved experimentally with a bandwidth of 48 MHz. Figure 7 shows the simulated and experimental S parameter versus frequency curves for the designed antenna in free space and a muscle environment. A resonant frequency in the range of the ISM band i.e. 2.45~2.5 GHz is achieved for all three conditions. The return loss is degraded somewhat by the implantation of the antenna into the chicken tissue. After introducing DGS, transition sharpness increased, higher harmonics were suppressed and, pass band and stop band characteristics improved. These results are observed clearly in the S-parameter curve for the antenna with DGS in Fig. 8. It exhibits a large bandwidth of 900 MHz for WiMAX application with a low return loss of -45 dB.
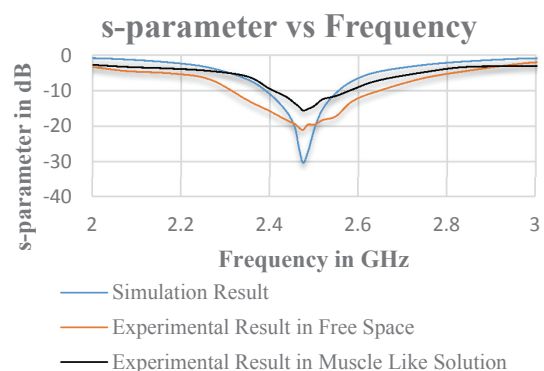

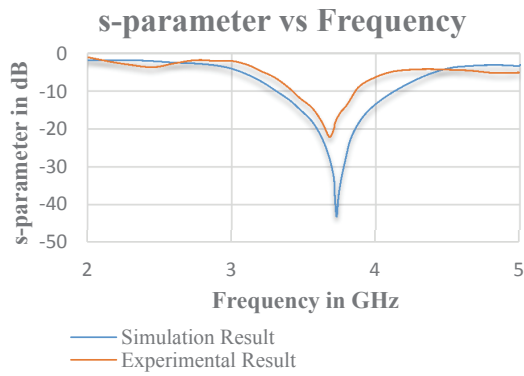Fig. 7. S_{11} parameter of the proposed antenna for implantation.

s-parameter vs Frequency

Fig. 8. S$_{11}$ parameter of the proposed antenna with DGS for Wi-MAX application.

4.3 Radiation pattern and three-dimensional current distribution

The radiation pattern is the plot between powers radiated by an antenna as a function of the direction away from the antenna. It is usually expressed in terms of an azimuthal component and an elevation component of the radiation pattern. The azimuthal component is an E$_\phi$ component and the elevation component is an E$_\theta$ component of the electric field polar plot as shown in Figs. 9 and 10. Simulated radiation patterns for both the antennas in the *XZ* and *YZ* planes are obtained by using the Empire XCcel simulation tool. The *XZ* plane means that the angle ϕ is set at 0° and angle θ is varied, while the *YZ* plane means that the angle ϕ is set at 90°and θ is varied [16]. Figure 9 shows *XZ* plane polar plot and *YZ* plane polar plot for implantable antenna without DGS and Fig. 10 shows the *XZ* plane polar plot and the *YZ* plane polar plots for an antenna with DGS. The surface current distribution obtained through the simulation reveals the amount of current flow per unit area as shown in Fig. 11. Once the currents in the circuit are known, the electromagnetic fields can be computed. Figures 11(a) and 11(b) show current density at different positions on the patch antenna without and with DGS respectively. The amount of current flow can be calculated on any plane. Here, the current distribution is shown on the *XY* plane. Different colors are used for specifying the current density at different parts of the patch antenna, with red indicating the maximum current and blue the minimum current. Values for the current density in A/m^2 are shown in Fig. 11.
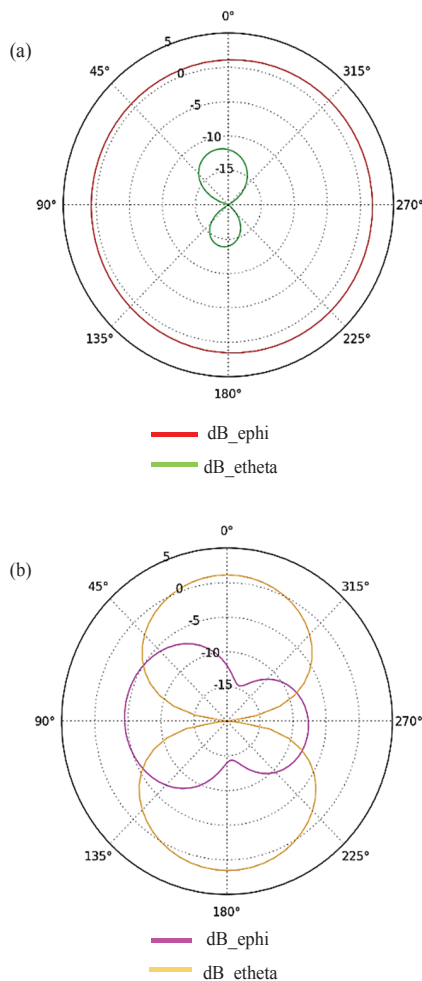

Fig. 9. Radiation pattern for implantable antenna without DGS (a) XZ plane and (b) YZ plane.
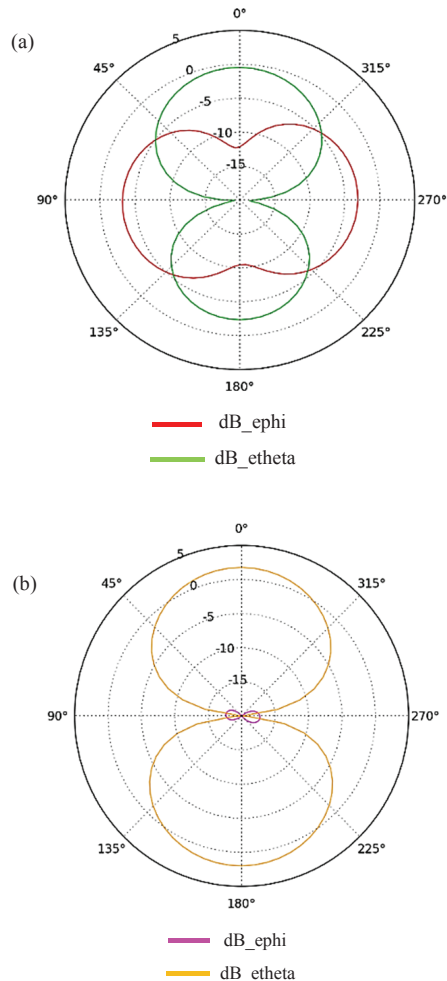

Fig. 10. Radiation pattern for antenna with DGS (a) XZ plane and (b) YZ plane.
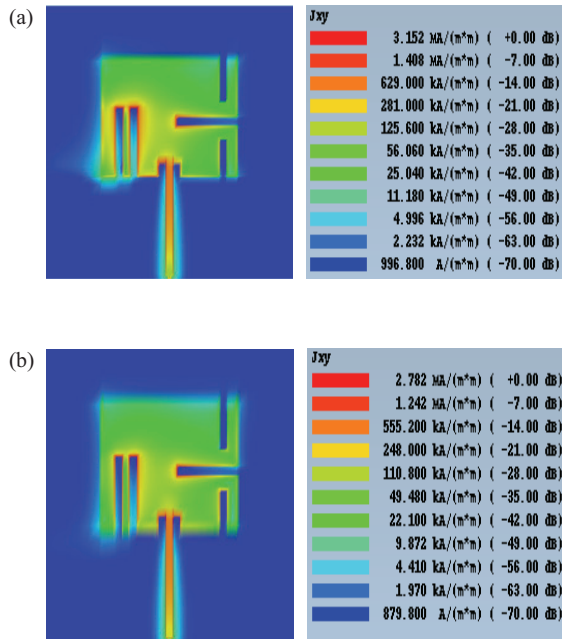
(a)

(b)

Fig. 11. Surface current distribution (a) implantable antenna without DGS and (b) Antenna with DGS.

5. CONCLUSIONS

In this paper, a slotted patch antenna with a compact size of 35 × 40 × 1.6 mm was proposed as a suitable implantable antenna for ISM band applications. Experimental results are obtained for an animal tissue to study the design in a realistic environment. The proposed antenna can be used for biomedical applications that require implantation. For implantation purpose the main challenge is miniaturization which was required as per the results obtained in this work. Furthermore, by introducing DGS, along with a slight variation in ground width, leads to WiMAX applications. Simulated and measured results show good agreement in both cases. Hence, these antennas can be used for biomedical and WiMAX applications.

REFERENCES

[1] S. A. Kumar, J. N. Sankar, D. Dileepan, and T. Shanmuganantham, *Trans. Electr. Electron. Mater.*, **16**, 250 (2015). [DOI: https://doi.org/10.4313/TEEM.2015.16.5.250]

[2] F. Merli, L. Bolomey, J. F. Zürcher, G. Corradini, E. Meurville, and A. K. Skrivervik, *IEEE Trans. Antennas Propag.*, **59**, 3544 (2011). [DOI: https://doi.org/10.1109/TAP.2011.2163763]

[3] C. Liu, Y. X. Guo, and S. Xiao, *IEEE Trans. Antennas Propag.*, **62**, 2407 (2014). [DOI: https://doi.org/10.1109/TAP.2014.2307341]

[4] A. Kiourti and K. S. Nikita, *IEEE Antenn. Propag. M.*, **54**, 210 (2012). [DOI: https://doi.org/10.1109/MAP.2012.6293992]

[5] F. Merli, L. Bolomey, F. Gorostidi, B. Fuchs, J. F. Zurcher, Y. Barrandon, E. Meurville, J. R. Mosig, and A. K. Skrivervik, *IEEE Antenn. Wireless Propag. Lett.*, **11**, 1650 (2012). [DOI: https://doi.org/10.1109/LAWP.2013.2238500]

[6] J. Kim and Y. Rahmat-Samii, *IEEE Trans. Microwave Theory Tech.*, **52**, 1934 (2004). [DOI: https://doi.org/10.1109/TMTT.2004.832018]

[7] A.A.S. Rabih, K. M. Begam, T. Ibrahim, and Z. A. Burhanudin, *Journal of Medical Research and Development*, **3**, 107 (2014).

[8] J. Liu, W. Y. Yin, and S. He, *Prog. Electromagn. Res.*, **107**, 115 (2010). [DOI: https://doi.org/10.2528/PIER10050904]

[9] L. H. Weng, Y. C. Guo, X. W. Shi, and X. Q. Chen, *Prog. Electromagn. Res. B*, **7**, 173 (2008). [DOI: https://doi.org/10.2528/PIERB08031401]

[10] P. V. Naidu and R. Kumar, *J. Microw. Optoelectron. Electromagn. Appl.*, **14**, 1 (2015). [DOI: https://doi.org/10.1590/2179-10742015v14i1422]

[11] K. Siakavara, *Microstrip Antennas* (INTECH, 2011). [DOI: https://doi.org/10.5772/14676]

[12] G. Breed, *High Frequency Electronics*, **7**, 50 (2008).

[13] E. Hanae, N. A. Touhami, M. Aghoutane, S. E. Amrani, A. Tazon, and M. Boussouis, *Prog. Electromagn. Res. C*, **55**, 25 (2014). [DOI: https://doi.org/10.2528/PIERC14092302]

[14] J. Gemio, J. Parron, and J. Soler, *Prog. Electromagn. Res.*, **110**, 437 (2010). [DOI: https://doi.org/10.2528/PIER10102604]

[15] U. M. Mc Carthy, G. Ayalew, F. Butler, K. Mc Donnell, J. Lyng, and S. Ward, *Agricultural Engineering International: CIGR Journal* (2009).

[16] W. Xia, K. Saito, M. Takahashi, and K. Ito, *IEEE Trans. Antennas Propag.*, **57**, 894 (2009). [DOI: https://doi.org/10.1109/TAP.2009.2014579]